Numerical modelling and experimental assessment of concrete spalling in fire

Manuchehr Shamalta,
TNO Centre for Fire Research, Delft, the Netherlands
Arnoud Breunese
TNO Centre for Fire Research, Delft, the Netherlands
Willy Peelen
TNO Civil Infrastructure, Delft, the Netherlands
Joris Fellinger
TNO Centre for Fire Research, Delft, the Netherlands

In this paper, the phenomenon of spalling of concrete in fire has been studied using a numerical model. Spalling is the violent or non-violent breaking off of layers or pieces of concrete when it is exposed to high temperatures as experienced in fires. The types and mechanisms of spalling have been explained. A numerical model has been developed, which takes into account main characteristics of the real phenomenon. To improve the stability, robustness and calculation time of the model analysis, the transport phenomenon and the mechanical behaviour have been coupled in a staggered way. The system of differential equations describing the transport phenomenon has been implemented in FEMLAB, an interactive environment to model single and coupled phenomenon based on partial differential equations. A one-dimensional example has been studied. It has been shown that the results are physically reasonable but still validation of the results needs to be done. These results will be validated against the experimental measurements and the results obtained by other recently developed models predicting the concrete spalling.

Key words: Concrete spalling, fire, high temperatures, porous medium, numerical modelling, staggered analysis

1 Introduction

A series of fires in road and rail tunnels have occurred across Europe over the past decade, causing a serious loss of life and significant structural damage. It was in the first place the human casualties and second the structural damage and as consequence the financial loss in the Mont Blanc tunnel, Tauern tunnel, Kaprun tunnel, Gotthard tunnel, Great Belt tunnel (during construction) and Channel tunnel (soon after commissioning) fires that have provided the impetus to take the fire safety more seriously. These unforgettable disasters seize the public attention, the European authorities attention and as consequence the engineers attention to focus on the fir safety.

As far as the fire safety is concerned the main structure shouldn't collapse until both rescue workers and users are safe. To this end it is important to know about the behaviour of the construction exposed to fire. The use of incombustible materials does not guarantee the safety of a structure. Steel, for instance, quickly loses its strength when heated and its yield strength decreases significantly as it absorbs heat, endangering the stability of the structure. Also reinforced concrete is not immune to fire. Concrete is the most widely used construction material on earth and has proved to be very durable under most conditions. Despite the fact that concrete has the advantages of durability in comparison to other construction materials, massiveness and in-combustibility related to fire safety, it can also undergo serious damages under fire conditions. Concrete may spall under elevated temperatures, exposing the steel reinforcement and weakening structural members.

Spalling of concrete is currently a hot issue in civil engineering and it is indicated as the major cause for non-recoverable damage in structures subjected to fire. Figure 1 shows the construction damage that occurred due to the fire inside the Channel tunnel. The concrete was completely destroyed and vanished leaving only the bare steel reinforcement which lost it's strength and bent down in the intense heat. This fire caused huge finance damage but fortunately no lives were lost.

Figure 1. Fire damage in Channel tunnel

Spalling of concrete is the violent or non-violent breaking off of layers or pieces of concrete from the surface of a structural element when it is exposed to high temperatures as expected in fires. Spalling of concrete has serious consequences. Loss of section (i.e. reduction of the cross-sectional area of the concrete so that it is no longer able to sustain the stresses) and loss of protection to steel reinforcement (reinforcement reaching excessive temperatures) lead to a decrease of the structural load bearing capacity and ultimately failure.

In this paper, a model is employed to describe the phenomenon of spalling of concrete due to high temperatures. The concrete is modelled as a three-phase porous medium with constituents

in the solid phase (solid matrix and chemically bound water), the liquid phase (capillary or free water and physically adsorbed water) and the gas phase (dry air and water vapour). This model also takes into account the phase changes of water.
The governing differential equations describing the equilibrium of the flow of mass, energy and momentum have been obtained based on the mixture theory by fully integration of the energy and mass conservation equations. Four primary state variables, i.e. gas pressure p_g, capillary pressure p_c, temperature T and displacement vector of the solid matrix $\mathbf{u}$, were chosen to describe the state of concrete at high temperatures. After introducing the constitutive relationships and the thermodynamic state relationship a system of differential equation of four coupled partially differential equations was found. Three of them (p_g, p_c and T) describe the transport phenomenon and the fourth one ($\mathbf{u}$) describes the mechanical behaviour of the system. This paper describes the fully coupled system. However, for the implementation of the model, the transport phenomenon and the mechanical behaviour are coupled in a staggered way. It means that the effect of the transport parameters on the mechanical behaviour is considered but the influence of the mechanical behaviour on the transport phenomena is assumed to be negligible. Staggered analysis of this system has several advantages. First of all the analysis will be more stabile and robust. Second, the calculation time will be decreased by choosing different discretisations in time and space to calculate the transport parameters than that to calculate the displacements.
The differential equations describing the transport phenomenon was solved using the computer programme FEMLAB. A one-dimensional example was studied. In the frame of this example the temperature and pressures were calculated inside an concrete wall exposed to fire at one side. The results were plotted for different saturation degrees of the concrete. Next development within the framework of this project is to validate these results.
The validation will be done firstly using experimental results and secondly by comparison with the results obtained by another recently developed numerical model [3] describing the phenomenon spalling of concrete.

2 Mechanisms which lead to spalling

Spalling can be grouped into five categories violent spalling, sloughing-off, corner spalling, explosive spalling and post-cooling spalling [1].
Many material (e.g. aggregate type), geometric (e.g. section shape and size), productional (e.g. casting process) and environmental (e.g. heating rate) factors have been identified from experiments as influencing spalling of concrete in fire. The main factors influencing spalling are the heating rate, permeability of the material, initial pore saturation level and the level of external applied load. High strength concrete is more likely to explosively spall than normal strength concrete despite its higher tensile strength. This is because of the lower ductility and the greater pore pressures that build up during heating owing to the material's lower

permeability. Other factors such as the cross sectional size and shape, heating profile, concrete age, aggregate size and type, the presence of cracking and reinforcement also play a role.
Each kind of concrete spalling is caused by a specific combination of physical or chemical mechanisms. These are as follows:

- Pore pressure rises due to expanding and evaporating water at elevated temperatures;
- Compression of the heated surface due to a thermal gradient in the cross section;
- Internal cracking due to difference in thermal expansion between aggregate and cement paste;
- Cracking due to difference in thermal expansion/deformation between concrete and reinforcement bars;
- Strength loss due to chemical transitions during heating.

Violent spalling which is separation of small or large pieces of concrete from the cross section, is caused by pore pressure, thermal gradients and internal cracking. Sloughing-off spalling is caused by strength loss due to internal cracking and chemical deterioration of the cement paste. Corner spalling is caused by cracks due to the different thermal deformation of concrete and reinforcement bar at the corner of concrete. Explosive spalling is the result of the combination of the pore pressure and thermal gradients in the cross-section. Post-cooling spalling occurs after the fire is over and caused by internal cracking due to different thermal expansion of aggregate and loss of strength due to chemical transitions.

3 Numerical approach

3.1 ***General overview***

To study the phenomenon concrete spalling in fire a fully coupled multi-phase hydro-t hermal-mechanical model is considered, which takes into account the main characteristics of this problem. Within this model the concrete is considered to be a three phase porous medium based on mixture theory or averaging theory. This theory offers possibilities for a better understanding of the microscopic situation and its relation to the macroscopic level. The three considered phases within this model are solid phase, liquid phase and gas phase. The solid phase consists of solid matrix and chemically bound water. The liquid phase consists of capillary or free water and physically adsorbed water. Physically adsorbed water is present in the hole range of water contents of the medium, while, the capillary or free water appears when water content exceeds the so-called solid saturation point S_{ssp} [6]. The gas phase is a mixture of dry air and water vapour.
Transitions that take place between the three abovementioned phases can be physical or chemical in nature and are thermodynamically not fully reversible. In cement based concrete these phase changes are dehydration/hydration of chemically bound water, evaporation/condensation of free water and desorption/adsorption of physically adsorbed water. Other phase changes such as the decarbonation/carbonation and α-β inversion/ β-α inversion (α-β transformation of quartz at 573 °C) were not incorporated within this model.

It has also been assumed that the phase changes happen only between water vapour and the other three, i.e. there is no direct mutual exchange between chemically bound water, physically adsorbed water and capillary water. Figure 2 shows schematically the phase changes of water implemented in model.

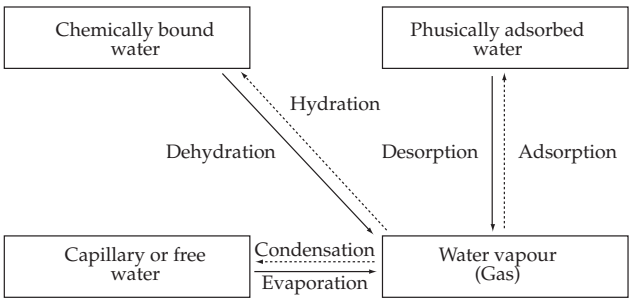

Figure 2. Phase changes of water; solid arrows indicate energy consumption, dashed arrows indicate energy release

One can see in this figure that dehydration is the phase change of chemically bound water to water vapour which is an energy consuming chemical process. This process produces a reduction in the solid skeleton mass of the cement paste. Hydration, which is a reverse process of dehydration, takes place at room temperature and the process increases with temperature in the presence of moisture up to 80 ˚C or more resulting in an increase in the mass of solid skeleton. Above this temperature, dehydration is a gradual process up to 850 ˚C [7]. Evaporation is the process by which water gains energy to change from the capillary or free water to the gas phase. In contrary, condensation is the process whereby water vapour is returned to the liquid phase. Desorption is the evaporation of water molecules from the surface of the solid, gaining energy, while, adsorption is the binding of the water molecules to the surface of the solid. Evaporation of water increases with temperature particularly above approximately 80 ˚C depending on the pressure. The loss of the capillary water does not significantly influence the mechanical property of the cement paste but the loss of physically adsorbed water has a major influence on the mechanical properties. Beyond the triple point of water (374.14 ˚C) no difference exists anymore between capillary water and water vapour. Also the capillary pressure vanishes.

The basic equations used in this model fall under three main categories: a) constitutive relationship of concrete describing the real behaviour of the material derived directly from experiments, b) thermodynamic state equations allowing the treatment of dry air and moist air as ideal gases (Clapeyron's law) as well as equilibrium relations for capillary menisci (Kelvin's law) and gas phases (Dalton's law) c) general laws of conservation which must be obeyed in space and time including the first principle of thermodynamics (enthalpy conservation).

Before these equations are discussed, first the definition of the material time derivative is given.

3.2 ***Constitutive relationship and thermodynamic state relationships***

In this model we assume the moist air as a mixture of two ideal gases, i.e. dry air and water vapour. The equations of state of a perfect gas, applied to dry air (g_a), vapour (g_w) and moist air (g) are

$$p_{ga} = \rho_{ga}\frac{RT}{M_a}, p_{gw} = \rho_{gw}\frac{RT}{M_w}, \rho_g = \rho_{ga} + \rho_{gw}, p_g = p_{ga} + p_{gw}, \frac{1}{M_g} = \frac{\rho_{gw}}{\rho_g}\frac{1}{M_{gw}} + \frac{\rho_{ga}}{\rho_g}\frac{1}{M_{ga}} \tag{1}$$

where $M\pi$, $\rho\pi$ and $p\pi$ are the molar mass, the density and pressure of constituent π, respectively, and R is the universal gas constant. The degree of saturation of constituent π is defined as the ratio of the volume of constituent π to the volume of the void. It follows immediately for the saturation degree of liquid water and the gas that

$$S_w + S_g = 1. \tag{2}$$

The degree of saturation with liquid water is an experimentally determined function of capillary pressure p_c and temperature T. This function is usually presented in the form of the sorption isotherms [2,3].

The capillary pressure is defined as the pressure difference between the gas phase and the liquid phase, which can be find through the Laplace equation from the pore radius r and the surface tension σ

$$p_c = p_g - p_w = \frac{2\sigma}{r} \tag{3}$$

and the pressure in the solid phase is

$$S_w + S_g = p_c = p_g - p_w = p_s = p_w S_w + p_g S_g = p_g - p_c S_w \tag{4}$$

where $S\pi$ is the saturation degree of the constituent π.

For the density of water many experiments were carried out in the past. The values were approximated by a linearization in temperature and pressure:

$$\rho_w = \rho_{wo}\exp\left(-\beta_w\left(T - T_o\right) + C_w\left(p_w - p_{wo}\right)\right) \tag{5}$$

where ρ_{wo} is the water density at the reference temperature T_o and pressure ρ_{wo}, β_w is the thermal expansion coefficient and C_w is the compressibility coefficient.

For the relationship between the relative humidity (RH) and the capillary pressure in the pores, the Kelvin-Laplace law is assumed to be valid

$$RH = \frac{p_{gw}\left(T\right)}{p_{gws}\left(T\right)} = \exp\left(\frac{p_c M_w}{\rho_w RT}\right), \tag{6}$$

with $p_{gws}(T)$ the water vapour saturation pressure which can be calculated using the Clausous-Clapeyron equation,

$$p_{gws}\left(T\right) = p_{gwso}\exp\left(-\frac{M_w \Delta H_{gw}}{R}\left(\frac{1}{T}-\frac{1}{T_o}\right)\right), \tag{7}$$

where p_{gwso} is the water vapour pressure at reference temperature T_o and ΔH_{gw} is the specific enthalpy of evaporation.
Darcy's law is assumed valid for transport of both water and gas in slow phenomenon.

$$\mathbf{v}_{\pi s} = \frac{k_{r\pi}\boldsymbol{\kappa}}{nS_\pi \mu_\pi}\left(-\nabla p_\pi + \rho_\pi \mathbf{g}\right). \tag{8}$$

In this relation κ is the permeability tensor of the medium, μ_π is the dynamic viscosity of the constituent π, n is the porosity and $k_{r\pi}$ is the relative permeability. The porosity n is defined as the ratio of the volume of the void to the total volume of the medium
Diffusive-dispersive mass flux Jpa is governed by Fick's law

$$\mathbf{J}_{\pi\alpha} = nS_\pi \rho_\alpha \mathbf{v}_{\pi\alpha} = -\rho_\alpha \mathbf{D}_{\pi\alpha}\nabla\left(\frac{\rho_\pi}{\rho_\alpha}\right) \tag{9}$$

where $\mathbf{D}_{\pi\alpha}$ is effective dispersion tensor, π is the diffusion phase and a is the phase in which diffusion takes place (α=w,g).
A constitutive assumption for the heat flux is the generalised version of Fourier's law, $\mathbf{q}$=-$\lambda_{eff}\Delta T$, with λ_{eff} the effective thermal conductivity tensor and $\mathbf{q}$ the heat flux of the multiphase medium, the sum of the partial heat fluxes $\mathbf{q}_\pi$. For porous media the following linear relationship may be used [8]:

$$\lambda_{eff} = \lambda_{dry}\left(1 + 4\frac{nS_w \rho_w}{\left(1-n\right)\rho_s}\right). \tag{10}$$

3.3 ***Governing equations***

To find the governing equations we need to fully integrate the conservation equations of the three quantities, mass, energy and momentum (force balance). These conservation equations can be derived using the general conservation equation. For a generic conserved variable ψ (e.g. like mass, momentum and energy) the general conservation equation may be written as

$$\frac{\partial \psi}{\partial t} + \nabla \cdot \left(\mathbf{f} + \psi \mathbf{v} \right) - H = 0 \quad , \tag{11}$$

with **f** the flux of ψ in the absence of the fluid transport, ψ**v** the transport flux and H the source or sink of ψ. Given equation (11) for the conservation of anything and specifying the subscript s for solid, w for liquid phase and g for the gas phase (dry air plus vapour), it is now straightforward to consider the conservation equations.

To derive the conservation equation of solid mass we just substitute $\psi = (1\text{-}n)\rho_s$ (density is amount of mass per unit volume), **f = 0** (mass flux can only change due to transport) and $_{\mathrm{H}} = -\partial\,(m_{dehydr})/\partial t$ (solid mass can change by dehydration/hydration process) into equation (11) to get

$$\frac{\partial \left(\left(1-n \right) \rho_s \right)}{\partial t} + \nabla \cdot \left(\left(1-n \right) \rho_s \mathbf{v}_s \right) = -\dot{m}_{dehydr} \quad . \tag{12}$$

The mass conservation equations of liquid water, vapour water and dry air can be derived in the same way as equation (12) by substitution $H = -\partial\,(m_l)/\partial t$ for liquid water (mass of liquid water can be change by eider evaporation/condensation or desorption/adsorption processes), $H = \partial\,(m_{dehydr} + \mathrm{ml})/\partial t$ for vapour water (mass of vapour water can be change by dehydration/hydration, evaporation/condensation and desorption/adsorption processes) and $H = 0$ (dry air can not be crated or destroyed) for dry air into (11). Hence, one may find for mass balance equation of liquid water

$$\frac{\partial \left(nS_w \rho_w \right)}{\partial t} + \nabla \cdot \left(nS_w \rho_w \mathbf{v}_w \right) = -\dot{m}_l \quad , \tag{13}$$

for mass balance equation of vapour water

$$\frac{\partial \left(nS_g \rho_{gw} \right)}{\partial t} + \nabla \cdot \left(nS_g \rho_{gw} \mathbf{v}_{gw} \right) = \dot{m}_{dehydr} + \dot{m}_l \quad , \tag{14}$$

and for mass balance equation of dry air

$$\frac{\partial\left(nS_g\rho_{ga}\right)}{\partial t}+\nabla\cdot\left(nS_g\rho_{ga}\mathbf{v}_{ga}\right)=0 \tag{15}$$

The amount of heat (energy) per unit volume is $\psi=(\rho C_p)_{eff}T$ where C_p is the specific heat, T is the temperature and $(\rho C_p)_{eff}$ is the effective thermal capacity of partially saturated concrete. The heat flux has two components due to conduction and transport. In the absence of transport the heat flux is $\mathbf{f}=-\lambda_{eff}\nabla T$ where λ_{eff} is the effective thermal conductivity of partially saturated concrete. Finally, heat can be released/absorbed during dehydration/hydration, evaporation/condensation and desorption/adsorption. The of energy related to the phase changes is equal to the change in the enthalpy, ΔH. Thus the heat released/absorbed during abovementioned processes may be calculated as $H=\Delta H_{dehydr}\partial(m_{dehydr})/\partial t+\Delta H_l\partial(m_l)/\partial t$. Hence, the energy conservation equation may be written as follows:

$$\left(\rho C_p\right)_{eff}\frac{\partial T}{\partial t}+\left(\rho_w C_{pw}\mathbf{v}_w+\rho_g C_{pg}\mathbf{v}_g\right)\cdot\nabla T-\nabla\cdot\left(\lambda_{eff}\nabla T\right)=\dot{m}_{dehydr}\Delta H_{dehydr}+\dot{m}_l\Delta H_l. \tag{16}$$

In these equations $l=desorp$ if $S\le S_{ssp}$ and $l=evap$ if $S>S_{ssp}$.
Conservation of linear momentum or force balance can be derived in exactly the same way, however momentum is a vector field. In general momentum is $m\mathbf{v}$, therefore the amount of momentum per unit volume is $\psi=(1-n)\rho_s\mathbf{v}_s$ for solid phase, $\psi=nS_w\rho_w\mathbf{v}_l$ for liquid water phase, $\psi=nS_g\rho_{gw}\mathbf{v}_{gw}$ for vapour water phase and $\psi=nS_g\rho_{ga}\mathbf{v}_{ga}$ for dry air phase. The momentum can be changed by forces. As stress is simply force per unit area, the stress can also be thought of as a flux of the force potential, i.e. $\mathbf{f}=-(1-n)\boldsymbol{\sigma}_s$ for solid phase, $\mathbf{f}=-nS_w\boldsymbol{\sigma}_w$ for liquid water phase, $\mathbf{f}=-nS_g\boldsymbol{\sigma}_{gw}$ for vapour water phase and $\mathbf{f}=-nS_g\boldsymbol{\sigma}_{ga}$ for dry air phase. The other forces are body forces such as gravity and internal forces. Neglecting the internal forces and considering the change of linear momentum due to dehydration/hydration, evaporation/condensation and desorption/adsorption processes, thus $H=(1-n)\rho_s\mathbf{g}-[\partial(m_{dehydr})/\partial t]\mathbf{v}_s$ for solid phase, $H=nS_w\rho_w\mathbf{g}-[\partial(m_l)/\partial t]\mathbf{v}_w$ for liquid water phase, $H=nS_g\rho_{gw}\mathbf{g}+[\partial(m_{dehydr})/\partial t+\partial(m_l)/\partial t]\mathbf{v}_{gw}$ for vapour water phase and $H=nS_g\rho_{ga}\mathbf{g}$ for dry air phase where $\mathbf{g}$ is the net acceleration. Substituting into (11) yields

$$\frac{\partial\left(\left(1-n\right)\rho_s\mathbf{v}_s\right)}{\partial t}+\nabla\cdot\left(\left(1-n\right)\rho_s\mathbf{v}_s\otimes\mathbf{v}_s\right)-\nabla\cdot\left(\left(1-n\right)\boldsymbol{\sigma}_s\right)-\left(1-n\right)\rho_s\mathbf{g}+\dot{m}_{dehydr}\mathbf{v}_s=0 \tag{17}$$

$$\frac{\partial\left(nS_w\rho_w\mathbf{v}_l\right)}{\partial t}+\nabla\cdot\left(nS_w\rho_w\mathbf{v}_w\otimes\mathbf{v}_w\right)-\nabla\cdot\left(nS_w\boldsymbol{\sigma}_w\right)-nS_w\rho_w\mathbf{g}+\dot{m}_l\mathbf{v}_w=0 \tag{18}$$

$$\frac{\partial\left(nS_g\rho_{gw}\mathbf{v}_{gw}\right)}{\partial t}+\nabla\cdot\left(nS_g\rho_{gw}\mathbf{v}_{gw}\otimes\mathbf{v}_{gw}\right)-\nabla\cdot\left(nS_g\sigma_{gw}\right)-nS_g\rho_{gw}\mathbf{g}-\left(\dot{m}_{delvydr}+\dot{m}_l\right)\mathbf{v}_{gw}=0 \tag{19}$$

$$\frac{\partial\left(nS_g\rho_{ga}\mathbf{v}_{ga}\right)}{\partial t}+\nabla\cdot\left(nS_g\rho_{ga}\mathbf{v}_{ga}\otimes\mathbf{v}_{ga}\right)-\nabla\cdot\left(nS_g\sigma_{ga}\right)-nS_g\rho_{ga}\mathbf{g}=0 \tag{20}$$

for solid, liquid water, vapour water and dry air phase, respectively. Expanding the first and second terms of equations (17)-(20) and summation of these equations and by substitution of equations (12)-(15) into the result yield to the following conservation of momentum

$$\begin{aligned}\nabla\cdot\sigma+\rho\mathbf{g}=&\left(1-n\right)\rho_s\left(\frac{\partial\mathbf{v}_s}{\partial t}+\mathbf{v}_s\nabla\cdot\left(\mathbf{v}_s\right)\right)+nS_w\rho_w\left(\frac{\partial\mathbf{v}_w}{\partial t}+\mathbf{v}_w\nabla\cdot\left(\mathbf{v}_w\right)\right)\\&+nS_g\rho_{gw}\left(\frac{\partial\mathbf{v}_{gw}}{\partial t}+\mathbf{v}_{gw}\nabla\cdot\left(\mathbf{v}_{gw}\right)\right)+nS_g\rho_{ga}\left(\frac{\partial\mathbf{v}_{ga}}{\partial t}+\mathbf{v}_{ga}\nabla\cdot\left(\mathbf{v}_{ga}\right)\right)\end{aligned} \tag{21}$$

where ρ is the average density of the multiphase medium, given by $\rho=(1-n)\rho_s+nS_w\rho_w+nS_g\rho_g$ and σ the total stress of the multiphase medium, expressed by $\sigma=(1-n)\sigma_s+nS_w\sigma_w+nS_g\sigma_g$. In which σ_s, σ_w and σ_g are the intrinsic stresses and can be calculated by:

$$\sigma_s=\sigma-\alpha\mathbf{I}p_s,\sigma_w=\mathbf{I}p_w,\sigma_g=\mathbf{I}p \tag{22}$$

with $\mathbf{I}$ the identity tensor, $\sigma'=\mathbf{D}_e\varepsilon$ the effective stress and $\alpha=1-(K_s/K_M)$ is the Biot's constant with K_s and K_M the bulk moduli of solid and porous medium, matrix $\mathbf{D}_e$ is the stiffness matrix and $\varepsilon=\mathbf{Lu}$ the stress tensor, where $\mathbf{L}$ is the differential operator defined as follows:

$$\mathbf{L}=\begin{bmatrix}\frac{\partial}{\partial x}&0&0&\frac{\partial}{\partial y}&0&\frac{\partial}{\partial z}\\0&\frac{\partial}{\partial y}&0&\frac{\partial}{\partial x}&\frac{\partial}{\partial z}&0\\0&0&\frac{\partial}{\partial z}&0&\frac{\partial}{\partial y}&\frac{\partial}{\partial x}\end{bmatrix}^{\mathrm{T}} \tag{23}$$

Under the assumptions of small-strain theory and isothermal equilibrium and with neglecting the influence of the acceleration term $\partial\mathbf{v}/\partial_t$ and the convector terms $\mathbf{v}(\nabla.\mathbf{v})$, results for conservation of momentum

$$\nabla\cdot\sigma+\rho\mathbf{g}=\mathbf{0} \tag{24}$$

The conservation of angular momentum leads to the observation that the stress tensor is symmetrical.

3.4 ***Formulation of system of equations***

Applying the material time derivative to conservation equations (12)-(15) and expansion of the divergence terms in these equations one may find for solid mass conservation equation

$$\frac{(1-n)}{\rho_s}\frac{D_s\rho_s}{Dt}-\frac{D_s n}{Dt}+(1-n)\nabla\cdot\mathbf{v}_s=-\frac{\dot{m}_{dehydr}}{\rho_s} \tag{25}$$

for mass balance equation for liquid water

$$\frac{D_s n}{Dt}+\frac{n}{S_w}\frac{D_s S_w}{Dt}+\frac{n}{\rho_w}\frac{D_s\rho_w}{Dt}+\frac{1}{S_w\rho_w}\nabla\cdot\left(nS_w\rho_w\mathbf{v}_{ws}\right)+n\nabla\cdot\mathbf{v}_s=\frac{-\dot{m}_l}{S_w\rho_w} \tag{26}$$

for mass balance equation for vapour water

$$\frac{D_s n}{Dt}+\frac{n}{S_g}\frac{D_s S_g}{Dt}+\frac{n}{\rho_{gw}}\frac{D_s\rho_{gw}}{Dt}+\frac{1}{S_g\rho_{gw}}\nabla\cdot\left(nS_g\rho_{gw}\mathbf{v}_{gs}\right)+\frac{1}{S_g\rho_{gw}}\nabla\cdot\left(nS_g\rho_{gw}\mathbf{v}_{gwg}\right)+n\nabla\cdot\mathbf{v}_s=\frac{\dot{m}_{dehydr}+\dot{m}_l}{S_g\rho_{gw}}, \tag{27}$$

for mass balance equation for dry air

$$\frac{D_s n}{Dt}+\frac{n}{S_g}\frac{D_s S_g}{Dt}+\frac{n}{\rho_{ga}}\frac{D_s\rho_{ga}}{Dt}+\frac{1}{S_g\rho_{ga}}\nabla\cdot\left(nS_g\rho_{ga}\mathbf{v}_{gs}\right)+\frac{1}{S_g\rho_{ga}}\nabla\cdot\left(nS_g\rho_{ga}\mathbf{v}_{gag}\right)+n\nabla\cdot\mathbf{v}_s=0 \tag{28}$$

The first term in equation (25) that is related to the material time derivative of the solid density. The solid density ρ_s has been considered as function of solid pressure p_s, temperature T, the first invariant of effective stress tensor $\mathrm{tr}\sigma'$ and the degree of cement dehydration Γ_{dehydr}. Thus its derivative with respect to time t leads to:

$$\frac{1}{\rho_s}\frac{D_s\rho_s}{Dt}=\frac{1}{\rho_s}\left(\frac{\partial\rho_s}{\partial p_s}\frac{D_s p_s}{Dt}+\frac{\partial\rho_s}{\partial T}\frac{D_s T}{Dt}+\frac{\partial\rho_s}{\partial\mathrm{tr}\boldsymbol{\sigma}'}\frac{D_s\mathrm{tr}\sigma'}{Dt}+\frac{\partial\rho_s}{\partial\Gamma_{dehydr}}\frac{D_s\Gamma_{dehydr}}{Dt}\right) \tag{29}$$

However $\frac{1}{\rho_s}\frac{\partial\rho_s}{\partial p_s}=\frac{1}{K_s}, \frac{1}{\rho_s}\frac{\partial\rho_s}{\partial T}=-\beta_s, \frac{1}{\rho_s}\frac{\partial\rho_s}{\partial\mathrm{tr}\sigma}=\frac{1}{3(n-1)K_s}$ and

$\frac{D_s\Gamma_{dehydr}}{Dt}=-3(1-\alpha)K_s\left(\nabla\cdot\mathbf{v}_s+\frac{1}{K_s}\frac{D_s p_s}{Dt}-\beta_s\frac{D_s T}{Dt}\right)$ in which K_s is the bulk modulus of solid, β_s

is the thermal expansion coefficient of solid and a is the Biot's constant. Substitution of these expressions into relation (29) gives

$$\frac{1}{\rho_s}\frac{D_s\rho_s}{Dt}=\frac{1}{1-n}\left(\frac{\alpha-n}{K_s}\frac{D_sp_s}{Dt}-(\alpha-n)\beta_s\frac{D_sT}{Dt}-(1-\alpha)\nabla\cdot\mathbf{v}_s+\frac{1-n}{\rho_s}\frac{\partial\rho_s}{\partial\Gamma_{dehydr}}\frac{D_s\Gamma_{dehydr}}{Dt}\right) \tag{30}$$

Similarly, the third term in equation (26) that is related to the material time derivative of the water density can be obtained by assuming that ρ_w is a function of water pressure p_w and temperature T. Thus its derivative with respect to time t leads to:

$$\frac{1}{\rho_w}\frac{D_s\rho_w}{Dt}=\frac{1}{\rho_w}\left(\frac{\partial\rho_w}{\partial p_w}\frac{D_sp_w}{Dt}+\frac{\partial\rho_w}{\partial T}\frac{D_sT}{Dt}\right) \tag{31}$$

However $\frac{1}{\rho_w}\frac{\partial\rho_w}{\partial p_w}=\frac{1}{K_w}$ and $\frac{1}{\rho_w}\frac{\partial\rho_w}{\partial T}=-\beta_w$ in which K_w is the bulk modulus of water and

β_w is the thermal expansion coefficient of water. Hence equation (31) can be rewritten as:

$$\frac{1}{\rho_w}\frac{D_s\rho_w}{Dt}=\frac{1}{K_w}\frac{D_sp_w}{Dt}-\beta_w\frac{D_sT}{Dt} \tag{32}$$

Solving the material derivative of porosity n from equation (25) and substitution into the equations (26)-(28) and by introducing the relations (3)-(2), (8), (9), (30) and (32) into the results yield for mass balance equation for liquid water

$$S_w\left(\frac{\alpha-n}{K_s}+\frac{n}{K_w}\right)\frac{D_sp_g}{Dt}-S_w\left(\frac{\alpha-n}{K_s}S_w+\frac{n}{K_w}\right)\frac{D_sp_c}{Dt}+\alpha S_w\nabla\cdot\mathbf{v}_s-S_w\left((\alpha-n)\beta_s+n\beta_w\right)\frac{D_sT}{Dt}$$
$$+\left(n-\frac{\alpha-n}{K_s}S_wp_c\right)\frac{D_sS_w}{Dt}+\frac{1}{\rho_w}\nabla\cdot\left(nS_w\rho_w\mathbf{v}_{ws}\right)+S_w\frac{1-n}{\rho_s}\frac{\partial\rho_s}{\partial\Gamma_{dehydr}}\frac{D_s\Gamma_{dehydr}}{Dt}=-S_w\frac{\dot{m}_{dehydr}}{\rho_s}-\frac{\dot{m}_l}{\rho_w},$$

(33)

for mass balance equation for vapour water

$$S_g\frac{\alpha-n}{K_s}\frac{D_sp_g}{Dt}-S_gS_w\frac{\alpha-n}{K_s}\frac{D_sp_c}{Dt}+\alpha S_g\nabla\cdot\mathbf{v}_s-(\alpha-n)\beta_sS_g\frac{D_sT}{Dt}-\left(n+p_cS_g\frac{\alpha-n}{K_s}\right)\frac{D_sS_w}{Dt}$$
$$+\frac{1}{\rho_{gw}}\nabla\cdot\left(nS_g\rho_{gw}\mathbf{v}_{gs}\right)+\frac{1}{\rho_{gw}}\nabla\cdot\left(nS_g\rho_{gw}\mathbf{v}_{gwg}\right)+S_g\frac{n}{\rho_{gw}}\frac{D_s\rho_{gw}}{Dt}+S_g\frac{1-n}{\rho_s}\frac{\partial\rho_s}{\partial\Gamma_{dehydr}}\frac{D_s\Gamma_{dehydr}}{Dt}$$
$$=-S_g\frac{\dot{m}_{dehydr}}{\rho_s}+\frac{\dot{m}_{dehydr}+\dot{m}_l}{\rho_{gw}},$$

(34)

for mass balance equation for dry air

$$S_g \frac{\alpha - n}{K_s} \frac{D_s p_g}{Dt} - S_g S_w \frac{\alpha - n}{K_s} \frac{D_s p_c}{Dt} + \alpha S_g \nabla \cdot \mathbf{v}_s - S_g (\alpha - n) \beta_s \frac{D_s T}{Dt} - \left(n + p_c S_g \frac{\alpha - n}{K_s} \right) \frac{D_s S_w}{Dt}$$
$$+ \frac{1}{\rho_{ga}} \nabla \cdot \left(\rho_{ga} \frac{k_{rg} \mathbf{K}}{\mu_g} \left(-\nabla p_g + \rho_g \mathbf{g} \right) \right) + \frac{1}{\rho_{ga}} \nabla \cdot \left(n S_g \rho_{ga} \mathbf{v}_{gag} \right) + S_g \frac{n}{\rho_{ga}} \frac{\boldsymbol{D}_s \rho_{ga}}{Dt}$$
$$+ S_g \frac{1 - n}{\rho_s} \frac{\partial \rho_s}{\partial \Gamma_{dehydr}} \frac{D_s \Gamma_{dehydr}}{\boldsymbol{Dt}} = -S_g \frac{\dot{m}_{dehydr}}{\rho_s}.$$

(35)

Five partial differential equations (16), (24) and (33)-(35) form the system of differential equations of this problem. Choosing gas pressure p_g, capillary pressure p_c, temperature T and displacement vector of the solid matrix **u** as four primary state variables we need to eliminate one of equations. Solving the term $\partial (m_l)/\partial_t$ from equation (33) and with substitution in other equations, as well as the following relationships:

$$\nabla \cdot \mathbf{v}_s = \mathbf{IL} \frac{\partial \mathbf{u}}{\partial t}, \tag{36}$$

$$\frac{\partial S_w}{\partial t} = \frac{\partial S_w}{\partial p_c} \frac{\partial p_c}{\partial t} + \frac{\partial S_w}{\partial T} \frac{\partial T}{\partial t}, \tag{37}$$

$$\frac{\partial}{\partial t} \left(\frac{M_w}{TR} p_{gw} \right) = \frac{M_w}{RT} \frac{\partial p_{gw}}{\partial p_c} \frac{\partial p_c}{\partial t} + \frac{M_w}{RT} \left(\frac{\partial p_{gw}}{\partial T} - \frac{p_{gw}}{T} \right) \frac{\partial T}{\partial t} \tag{38}$$

$$\frac{\partial}{\partial t} \left(\frac{M_a}{TR} p_{ga} \right) = \frac{M_a}{RT} \frac{\partial p_g}{\partial t} - \frac{M_a p_g}{RT^2} \frac{\partial T}{\partial t} - \frac{M_a}{RT} \frac{\partial p_{gw}}{\partial p_c} \frac{\partial p_c}{\partial t} + \frac{M_a}{R\theta} \left(\frac{p_{gw}}{T} - \frac{\partial p_{gw}}{\partial T} \right) \frac{\partial T}{\partial t} \tag{39}$$

$$\nabla \left(\frac{p_{gw}}{p_g} \right) = \frac{1}{p_g} \frac{\partial p_{gw}}{\partial p_c} \nabla \boldsymbol{p}_c - \frac{p_{gw} \nabla p_g}{\left(p_g \right)^2} \tag{40}$$

and applying the Galerkin's method (weighted residuals) one can finally obtain the governing equations written in matrix form as follows:

$$\mathbf{C} \frac{\partial \mathbf{x}}{\partial t} + \mathbf{K} \mathbf{x} = \mathbf{F},$$

$$\text{with , } \mathbf{K} = \begin{bmatrix} \mathbf{K}_{gg} & \mathbf{K}_{gc} & \mathbf{K}_{gT} & \mathbf{0} \\ \mathbf{K}_{cg} & \mathbf{K}_{cc} & \mathbf{K}_{cT} & \mathbf{0} \\ \mathbf{K}_{Tg} & \mathbf{K}_{Tc} & \mathbf{K}_{TT} & \mathbf{0} \\ \mathbf{K}_{ug} & \mathbf{K}_{uc} & \mathbf{K}_{uT} & \mathbf{K}_{uu} \end{bmatrix}, \mathbf{C} = \begin{bmatrix} \mathbf{C}_{gg} & \mathbf{C}_{gc} & \mathbf{C}_{gT} & \mathbf{C}_{gu} \\ \mathbf{C}_{cg} & \mathbf{C}_{cc} & \mathbf{C}_{cT} & \mathbf{C}_{cu} \\ \mathbf{C}_{Tg} & \mathbf{C}_{Tc} & \mathbf{C}_{TT} & \mathbf{C}_{tu} \\ \mathbf{0} & \mathbf{0} & \mathbf{0} & \mathbf{0} \end{bmatrix} \text{ and } \mathbf{F} = \begin{Bmatrix} \mathbf{f}_g \\ \mathbf{f}_c \\ \mathbf{f}_T \\ \mathbf{f}_u \end{Bmatrix}.$$

The terms of the matrices **K**, **C** and **F** are presented in reference [9].

4 Staggered analysis of the problem

The coupled system of differential equations (41) can be solved numerically using the generalized method also known as the generalized midpoint role. In the model the transport phenomenon are coupled with the mechanical behaviour in staggered way. It is stated that the coupling terms, $\mathbf{C}_{gu}$, $\mathbf{C}_{cu}$ and $\mathbf{C}_{Tu}$ have relatively small influence to the solutions and are negligible. Still the effect of mechanical properties can be taken into account on the transport phenomena by an update of the transport parameters such as the permeability on the basic of the results of the previous steps in terms of mechanical stresses, strains and internal state variables such as cracks. This kind of coupling or staggered approach bring about some advantages. First of all the numerical stability of the analysis will be improved. For instance the transport phenomenon can be calculated using different elements than the mechanical behaviour. Second and as consequence of the first advantage the calculation time will be obviously decreased. Finally it will be possible to study the results easier and with more insight. The influence of parameters involved within this problem will be more obvious.
The objective is to couple the results obtained solving the transport phenomenon to already available and most sophisticated mechanical FEM models.
Up to now, calculations were performed of the coupled transport phenomena. Coupling to the mechanical behaviour is foreseen for 2005-2006.

5 Analysis of the numerical results

The coupled system of differential equation (41) describing only the transport phenomenon was solved numerically using the computer programme FEMLAB, an interactive environment to model single and coupled phenomenon based on partial differential equations. As a first attempt, the approach by Majorana et al [8], setting C_w=0 was followed. A one-dimensional example has been solved which deals with a concrete wall of 40 cm thickness. The initial conditions applied in this example at time instant $t=0$ are $p_g=p_{g0}$, $p_c=p_{c0}$, $T=T_0$. The Dirichlet boundary conditions are $p_g=p_{g0}$ on Γ_g, $p_c=p_{c0}$ on Γ_c, $T=T_0$ on Γ_T, and the Neumann boundary conditions are for the water flux (free water and vapour water) $q_w+q_{gw}=\beta_c(\rho_{gw}-\rho_{gw\infty})$ on Γ_w, for the gas flux $q_{ga}=0$ on Γ_g, for the heat transfer $q_T=\alpha_c(T-T\infty)$ on Γ_T. This wall has been subjected to transient heating from one side shown in Figure 3: (left). This Figure shows that temperature increases within very short time up to 1000 ˚C. at the other side the temperature is kept constant at T_0=20 ˚C. The main characteristic parameters of the material employed in the calculations are chosen from reference [6].

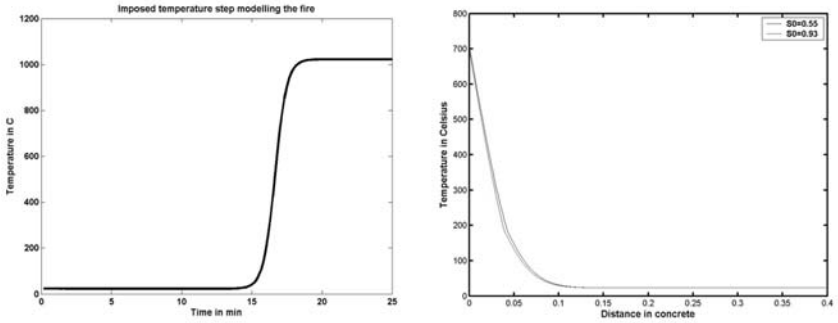

Figure 3. Imposed temperature (left) and temperature of the concrete wall after 26 minutes (right)

The problem is solved for two cases of different initial saturation degrees 55% and 93%. Figure 3: (right) shows the temperature in the concrete wall after about 26 minutes. This figure shows that during this time the initial temperature of the wall has changed with the minimum temperature as initial temperature and the maximum temperature about 700 °C. One can see in this figure that the difference between the temperatures for two different initial saturation degrees is very small. That means that so far the initial saturation degree hasn't too much influence on the temperature.

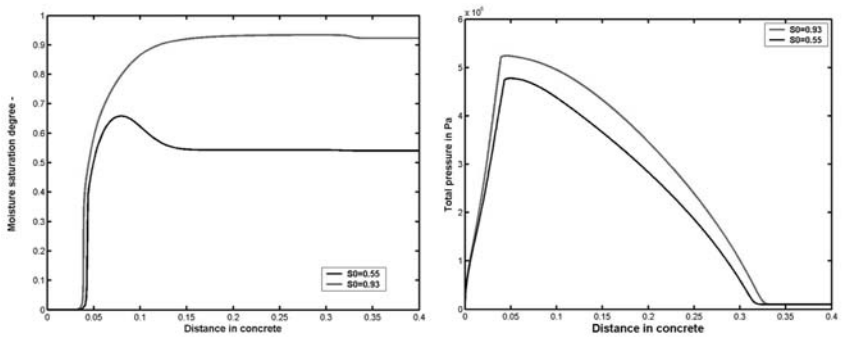

Figure 4. Saturation degree (left) and gas pressure in the concrete wall after 26 minutes (right)

The change of the saturation degree in the concrete wall is shown for both initial saturation degree in Figure 4: (left). This figure shows that the change of the saturation degree especially in the case of concrete with low initial saturation degree is considerable high. This change is even in contrast to temperature perceptible deep inside the concrete wall about 34 centimetre. One can see in Figure 4: (right) that the gas pressure is also changed as deep inside the wall as saturation degree.

6 Ongoing and future research

Validation of the model is the main part of this ongoing research. Previous to the validation, the material parameters will be improved and the staggered coupling of the transport phenomenon with the mechanical behaviour needs to be realised. In our ongoing and future work, we are focusing on the following challenges:

- Improving the material parameters and further implementation in FEMLAB;
- Coupling of the transport phenomenon calculated by FEMLAB with an FEM programme able to calculate the mechanical behaviour, for example DIANA;
- Comparison of the results of the final so-called staggered analysed system with the results of the other numerical programs such as HITECOSP [3], able to model the spalling of concrete;
- Validation of the results using the experimental results.

7 Conclusions

The phenomenon spalling of concrete at elevated temperatures was studied. Five manifestations of spalling of concrete were introduced. These are violent spalling, sloughing-off spalling, corner spalling, explosive spalling and post-cooling spalling. The mechanisms which lead to spalling have been explained. Pore pressure, thermal gradient, different thermal expansion between aggregate and cement paste, different thermal expansion between concrete and reinforcement bars and the change of the material properties due to temperature are the main factors influencing the spalling.
To analyse the phenomenon of concrete spalling a fully coupled multi-phase hydro-thermal-mechanical model was introduced, based on the existing hitecosp model [3]. Concrete was modelled as a three-phase porous material at high temperature. The three phases within this model are solid phase, liquid phase and gas phase. Phase changes are taken into account.
The constitutive relationships and the thermodynamic state equations describing the real behaviour of concrete were discussed. The governing equations that describe the behaviour of concrete as a three-phase porous material at high temperatures are presented. These equations were found by full integration of the mass, energy and momentum balance equations. The final form of the governing equations, choosing gas pressure p_g, capillary pressure p_c, temperature T and displacement vector of the solid matrix u as primary state variables, were derived. The coupled system of differential equations describing only the transport phenomenon coupling three gas pressure p_g, capillary pressure p_c and temperature T were solved using FEMLAB. A one-dimensional example has been solved which deals with a concrete wall exposed to a fast temperature rise up to 1000 ˚C. The temperature, saturation degree and gas pressure in the concrete wall have been presented for two different initial saturation degrees. These results are physically reasonable. It shows that inside concrete the

moisture content has a minor effect on the temperature distribution within the investigated range. The further steps of this research are firstly to improve the material parameters used within this model, second to couple this model to an FEM programme capable describing the mechanical behaviour and finally to validate the final results. The latest will be done using the experimental results and the results obtained by other recently developed models predicting the concrete spalling.

References

[1] R. W. Lewis and B. A. Schrefler, 'The Finite Element Method in the Static and Dynamic Deformation and Consolidation of Porous Media', Second Edition.

[2] Z. P. Bazant and W. Thonguthai, 'Pore pressure and drying of concrete at high temperature', J. Engng. Mech. Div. ASCE, 104, 1059-1079 (1978).

[3] D. Gawin, C. E. Majorana and B. A. Schreßer, 'Hygro- thermic and mechanical behaviour of concrete at high temperatures', in Advances in Computational Mechanics, Z. Wanxie, C. Gengdong and L. Xikui eds, Int. Academic Publishers, Beijing, 1996, pp. 221-242.

[4] A.J. Breunese and J.H.H. Fellinger, 'Tensile properties of concrete during fire', ECI Conference Advances in Cement and Concrete IX, Copper Mountain, Colorado, 10-14 August 2003.

[5] G. Khoury, C.E. Majorana, 'Modelling of concrete spalling in fire', 15th AIMETA Congress of Theoretical and Applied Mechanics, Taormina, 26-29 September 2001.

[6] Gawin, F. Pesavento, B.A. Schrefler, "Modelling of hygro-thermal behaviour of concrete at high temperature with thermo-mechanical and mechanical material degradation", CMAME, 192 (2003), 1731-1771.

[7] Harmathy, T. Z. 1970. Thermal Properties of Concrete at Elevated Temperatures. J. Materials (coden JMLSA), vol. 5, no. 1 (March), pp. 47-74. American Soc. Testing Mater.

[8] D. Gawin, C. E. Majorana and B. A. Schreßer, 'Numerical analysis of hygro-thermic and damage of concrete at high temperature', Mech. Cohes.-Frict. Mater. 4, 1999, 37-74.

[9] M. Shamalta, J. Fellinger, A. Breunese, W. Peelen, 'Numerical Modelling of Spalling of Concrete due to High Temperature' TNO-rapport 2004-CVB-R0379.